

백마시를 갖는 속도제어구동 시스템의 문제점

이 건 용

PROBLEMS OF A SPEED-CONTROLLED DRIVE SYSTEM WITH BACKLASH

K. LEE

FERNUNIVERSITÄT HAGEN, F.R. GERMANY

ABSTRACT In a speed-controlled system with cascade control which shows an optimal performance in the linear case, limit cycles can occur due to backlash. The various effects observed can be explained with the aid of the describing function. With a first-order load torque observer these limit cycles can be avoided. Moreover the dynamic performance improves considerably and the range of application of cascade control is extended.

INTRODUCTION

In this paper an elastic two-mass system with backlash is investigated to find out the reasons for limit cycles. Based upon this knowledge, a first-order load observer is proposed, as a simple measure, to improve cascade speed and position control. The results found by simulation were verified with an experimental setup with adjustable electrical and mechanical parameters.

The aims of publications dealing with backlash depend very much on the field of application. For the work presented here [1]-[3] were important contributions. The investigations which have been carried out and are continued are intended to lead to fundamental knowledge and new control concepts more than to a special solution.

MODELLING

A system as shown in Fig. 1 is investigated, consisting of two rotating masses (inertias θ_1 and θ_2) which are coupled via the backlash 2α , L_{12} as a nonlinear element, and via the linear torsion spring with the stiffness c_{12} . This spring represents the elasticity of a shaft, a gear etc. The inner friction of the elastic material is described by the linear damping d_{12} in parallel to the spring. Mass 1 is driven by a current-controlled dc or ac motor. A speed control loop and, in appropriate cases, a position control loop are superimposed to the current control loop (cascade structure). It is assumed that the variable to be controlled optimally is the speed n_2 of the load mass, but that only the motor quantities current i_1 and speed n_1 (and possibly α_1) can be measured. A constant torque m_2 is assumed acting on the load mass.

The transfer functions n_1/m_1 and n_2/m_1 of the controlled system (without current control) show a third order denominator which consists of an integral term and a second order lag.

$$\frac{n_1}{m_1} = \frac{1}{(q_1+q_2)p} \frac{1+p2d_{12}'/\omega_{012}+p^2/\omega_{02}^2}{H(p)} \quad (1)$$

$$\frac{n_2}{m_1} = \frac{1}{(q_1+q_2)p} \frac{1+p2d_{12}'/\omega_{02}+p^2/\omega_{012}^2}{N(p)} \quad (2)$$

$$H(p) = 1+p2d_{12}'/\omega_{012}+p^2/\omega_{012}^2 \quad (3)$$

$$\omega_{012} = \Omega_{012} T_H = \sqrt{\frac{c_{12}}{q_1 q_2 / (q_1 + q_2)}} \quad (4)$$

$$\omega_{02} = \Omega_{02} T_H = \sqrt{c_{12} / q_2} \quad (5)$$

$$d_{12}' = \frac{d_{12}}{2} \sqrt{\frac{1}{c_{12} q_1 q_2 / (q_1 + q_2)}} \quad (6)$$

$$d_2' = \frac{d_{12}}{2} \sqrt{\frac{1}{c_{12} q_2}} \quad (7)$$

$$q_1 = T_{\theta 1} / T_N \quad (8)$$

$$q_2 = T_{\theta 2} / T_N \quad (9)$$

$$T_N = 1 / \Omega_N \quad (10)$$

$$p = s T_N \quad (11)$$

According to industrial conditions the damping factor d_{12}' in Equ. (6) is assumed to be very small. Then the two poles in Eqs. (1) and (2) are conjugate complex.

Normally a PI speed controller is used and is optimized according to the Symmetrical Optimum (SO) which, however, applies in the case of real poles only. But if the condition $\Omega_{012} \geq 10\Omega_d$ holds, a transient performance as in Fig. 2 results. ($\Omega_d = 1/(2T_{gn})$) is the intersection angular frequency of the open speed control loop, with $T_{gn} = T_{e1} + T_{gn}$; standard values of the simulation are $T_{e1} = 5ms, T_{gn} = 2,7ms, \Omega_d = 64,65s^{-1}$). While the step response of n_1 and n_2 , Fig. 2, in its shape follows the SO standard response (the reference step not being smoothed), small oscillations of the two masses against each other occur. They originate from the weakly damped complex poles which cannot be influenced by a simple PI speed controller. With decreasing values $\Omega_{012} < 10\Omega_d$ the performance of n_2 is deteriorated. In the case of $\Omega_{012} = 0,1\Omega_d$ only n_1 follows the SO, but n_2 will oscillate, weakly damped. Then the system works like a one-mass oscillator with impressed speed n_1 , oscillating at Ω_{02} , Equ. (5). Only by means of a complete state feedback control all poles

could be shifted in such a way that optimal damping and time response of the controlled load speed n_2 is achieved.

DESCRIBING FUNCTION

If the reference value n_1 in Fig.1 is constant, $n_{1w}=n_{10} \neq 0$ and a constant load torque $m_2=m_{20} \neq 0$ acts on the mass m_2 , the system will obviously be able to run at constant speed $n_{20}=n_{10}=n_{w0}$. The question is, if this point of operation is asymptotically stable and which effects occur in no-load condition $m_2=0$.

Because of the high order of the system only a numerical treatment is possible in the time domain. Puzzling phenomena are observed in the case of step functions of n_1 : on the one hand the system comes to a new steady-state operation, on the other hand several stable limit cycles are possible. If, for example, m_2 is relatively low, a stable "big" limit cycle (Fig.3a) or a stable "small" limit cycle (Fig.3b) can develop. If m_2 is relatively high, no limit cycle occurs. Under certain conditions only one limit cycle is observed.

To understand these phenomena, it is helpful to realize that the nonlinearity acts like a switch which changes the structure of the system dependently on its input magnitude. If $\alpha_1 < \alpha_2$ becomes $\alpha_1 > \alpha_2$, the load mass is detached from the motor shaft and not longer controllable. If $\alpha_1 < \alpha_2$ becomes $\alpha_1 > \alpha_2$, motor and load mass get connected again. Sustained periodic oscillation, i.e. stable limit cycles, seem to be possible, if such impacts occur at suitable time intervals. The harmonic balance using the describing function of the backlash characteristic leads to a deeper understanding. The describing function is defined as $N_1 = x_{A1}/x_E = (R_{A1}/R_E) \exp(j\eta)$, if $x_E = R_E \exp(j\omega t)$ is the harmonic input quantity of the nonlinear characteristic and $x_{A1} = R_{A1} \exp(j(\omega t + \eta))$ is the first harmonic of the Fourier expansion of its output quantity.

If m_2 is kept constant, $m_2=m_{20}=\text{const.} \neq 0$, in steady-state condition $m_{12}=m_{20}=m_{20}$ holds. The torque m_{20} causes torsion of the spring. In this way a steady-state operating point is fixed on the backlash characteristic (Fig.4), producing non-symmetrical operating. The harmonic excitation of x_E requires a definite mean value x_{E0} (Fig.4.) in such a way that always $x_{A0}=m_{20}$ holds. A mean value $N = x_{A0}/x_{E0} = m_{20}$ of the describing function results. With the aid of the describing function the nonlinear backlash characteristic can be replaced through a linear gain $V_{12}=N_1$. As V_{12} is ≤ 1 , the spring c_{12} seemingly becomes "softer", the damping d_{12} becomes smaller. This harmonic linearization of the nonlinear element as means of testing stability requires the linear system to be a low-pass. This assumption is allowed, as will be proved by the results shown later on.

The stability of the nonlinear system can be investigated by analyzing the stability of the linearized system.

The pole configuration of Fig.6a reveals that a pair of conjugate complex and weakly damped poles is responsible for the instability. In the case of $V_{12}=1$ only small oscillations occur, as seen in Fig.2, which will decay. But with decreasing gain V_{12} these poles are shifted into the right half plane (Fig. 6), causing a building-up oscillation. The other poles of the system are not being influenced considerably through V_{12} .

In the nonlinear system, which is in steady-state operation, a sufficiently high disturbance induces "automatic" shifting of the weakly damped pair of poles into the right half plane. It depends on the amount of the load torque, if a stable limit cycle will occur or not.

This can be seen from Fig.4.2a. The crossings of the curves of the describing function and the stability margins represent possible limit cycles. The number of crossings depends on the

Parameter N_0/a , i.e. the per unit load torque m_{20}/α_{L12} of the system.

In the case of a very small load, $N_0/a=0.01$ for example, four crossings 1-4 exist in Fig.4.2a. To test the stability of these points, small deviations are assumed which lead to the arrow-head directions according to decreasing or increasing amplitudes of oscillation. The result is that only the points 2 and 3 describe stable limit cycles.

The following table can be derived, taking the minimum of the describing function $\text{MIN}(N_1)$ as criterion of the load:

Load case	$\text{MIN}(N_1)$	Limit cycles
1	$\text{MIN} = 0$	1 stable
2	$0 < \text{MIN} < V_{12L}$	2 stable
3	$\text{MIN} = V_{12L}$	1 stable and 1 semistable
4	$V_{12L} < \text{MIN} < V_{12H}$	1 stable
5	$\text{MIN} = V_{12H}$	1 semistable
6	$\text{MIN} > V_{12H}$	no limit cycle

In the case of no-load operation $m_{20}=0$ (case 1) only one stable limit cycle can occur. In the case of a relatively low load (case 2) either a "small" limit cycle (point 3 in Fig.4.2) or a "big" limit cycle (point 2) happens, depending on the magnitude of disturbance. This is the interpretation of the simulation results of Fig.3. In the case of a sufficiently high load (case 6) $m_{20}/\alpha_{L12} \gg 1.0$ the system shows total asymptotic stability of rest at each value $n_{20}=n_{10}=n_{w0}$. No limit cycle can occur.

These cases have been verified also experimentally with a speed controlled dc-machine and an elastically coupled load with adjustable values of backlash, elasticity and mass ratio.

This knowledge of the conditions of stability leads to various measures to avoid limit cycles, f.e.:

- (1) Design of a speed control with robustness against variation of V_{12} .
- (2) Use of a filter which flattens the resonance peaks in the region of instability
- (3) Compensation of the feedback of m_{12}

Measure (3) has been elaborated and applied successfully. Obviously the reaction of the weakly damped oscillator on the speed control loop via the shaft torque m_{12} is the reason of limit cycles. Due to the feedback of m_{12} the resonance peaks appear in the Bode diagram, corresponding to the pair of poles which cannot be damped sufficiently with a simple cascade control. If m_{12} was compensated completely through a counteracting torque of equal magnitude, the motor would be entirely decoupled from the reacting oscillator, and no resonance peaks could appear. But doing so, the damping of the oscillator could no longer be influenced through the speed control. Then the performance of the load speed n_2 would be highly unsatisfactory because of the weak damping d_{12} . For this reason only a partial compensation of m_{12} is successful.

This is done through a load torque observer shown in Fig.1. The torque m_{12} is being reconstructed from the measured motor current i_m , and the differentiated speed dn_1/dt , giving \hat{m}_{12} . This is fed to the current control loop via the gain K as an additional reference value. The observer may be realized also as a first-order Luenberger observer, being a network with integrator as shown in Fig.1. It is important to emphasize that this "integral observer" is completely equivalent to the "differential observer". As the observer time constant T_B normally is kept as low as possible (for example $T_B=1\text{ms}$), and as $T_B=T_{\theta 1}/k_B$ holds, k_B becomes correspondingly high. So the amplification of harmonics of the measured speed n_1 is equal with both networks.

it is a state variable, m_{12} , which is reconstructed by the observer and fed back to the system via the factor K . Transforming the PI speed controller into a state variable structure, a system with incomplete state variable feedback is received. Not all poles can be assigned arbitrarily by this method, but they can be influenced favourably. Assuming $T_D=0$ the Damping Optimum easily applies. Only two of the four double ratios of the approximated denominator polynomial, and the equivalent time constant of the closed-loop system can be predetermined. Assuming the values (in brackets) of Eqs. (4)-(10) systems with characteristic frequencies in the range of $25 \text{ Hz} < F_{012} < 100 \text{ Hz}$ show limit cycles. Observer parameters $K \approx 0.3$, $T_D \approx 1 \text{ ms}$ were found by simulation and experiment which prevent these limit cycles and provide a good dynamic performance in the range of $T_D/T_{\theta 1} = 0, 1, \dots, 10$. Though systems with $F_{012} < 25 \text{ Hz}$ are not able to limit cycling, their dynamics improves, if the observer is applied. Very "soft" systems, however, become slow. Complete state variable feedback is advisable then.

Linear system. In the case of a step function of the reference value n_1 , the settling time of n_2 is reduced by factor $\approx 0,8$ through the observer. In the case of a step function of the load torque m_2 , the settling time of n_2 is reduced by factor $\approx 0,75$, the maximum overshoot by factor $\approx 0,6$. Fig. 7 shows experimental results.

System with backlash. When the system is "softened" by the backlash (decreasing gain V_{12}), the observer flattens the resonance peaks, keeping them below the 0 db-margin (dashed curves in Fig. 5). The weakly damped pair of poles remains in the left half complex plane now (Fig. 6b). The system becomes asymptotically stable at each stationary operating point $n_{20} = n_{10} = n_{1w0}$ through the observer. The transient behaviour is quite similar to Fig. 7b shows, but n_2 is not controllable within the dead band.

CONCLUSIONS

The stability of a speed-controlled elastic two-mass system with backlash has been investigated with the describing function. Reasons and conditions for the existence of stable limit cycles were found. Based on this knowledge a first-order load torque observer is proposed. By this simple measure limit cycles are avoided, the dynamic performance of the system is improved and the cascade control can be applied, to a certain extent, also to "soft" mechanical systems

REFERENCES

- 1/ Ahrens, D., Raatz, E.: Regelungstechnische Untersuchung von Antrieben mit Kupplungs- oder Getriebeelose. Techn. Mitt. AEG-TELEFUNKEN 63 (1973), H. 6, S. 210-215.
- 2/ Wilharm, H.: Aufstellung und Einsatz von mathematischen Modellen für mechanische Systeme. Siemens Forsch.- u. Entw. Berichte Bd. 3 (1974), Nr. 5, S. 281D - 287D.
- 3/ Wilharm, H.: Erstellung des nichtlinearen Modells u. Folgeregelung für eine Vorschubachse bei Werkzeugmaschinen. VDI/VDE-Aussprachetag "Nichtlineare Regelsysteme", 1979.

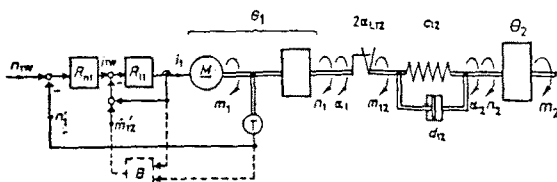


Fig. 1 Nonlinear speed-controlled two-mass system

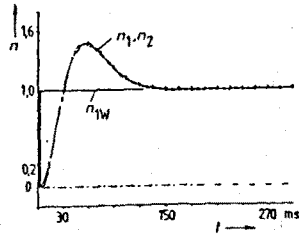


Fig. 2 Step response of the linear system (Simulation)

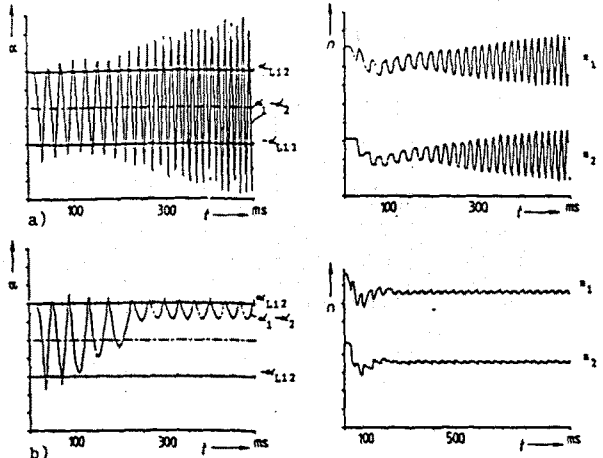
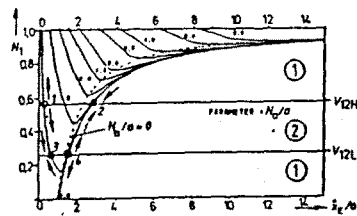
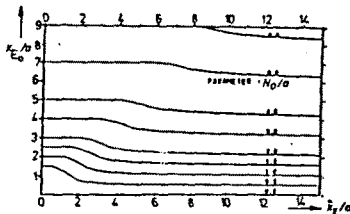


Fig. 3 Big limit cycle (a) and small limit cycle (b)



a) $N_1 = f(x_E, N_0, a)$



b) $X_{ED} = f(x_E, N_0, a)$

- ① Region of stability 1, 4 Instable limit cycles
- ② Region of instability 2, 3 Stable limit cycles

Fig. 4 Describing function of the backlash characteristic

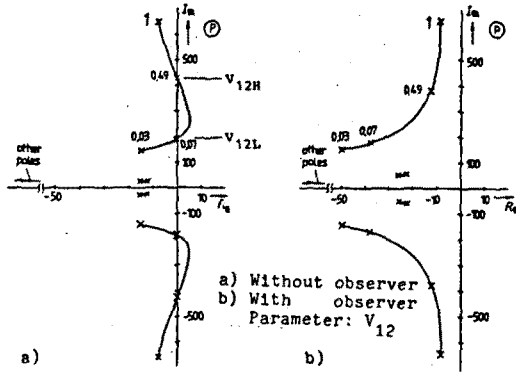
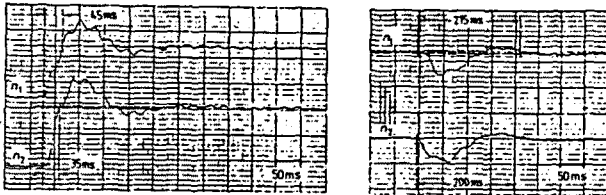
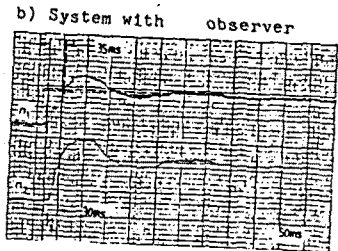
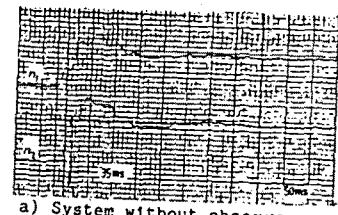


FIG. 5 Root locus of the closed-loop speed control



1 Reference step (n_{1w}) 2 Load step (m_2)
FIG. 6 Experimental results with the linear system
($\Omega_{012} = 207$ 1/s, $F_{012} = 32.9$ Hz)



Reference step (n_{1w})
FIG. 7 Experimental results with the nonlinear system